



Published in final edited form as:

*J Control Release*. 2012 October 10; 163(1): 25–33. doi:10.1016/j.jconrel.2012.06.007.

## Transport of Nanocarriers Across Gastrointestinal Epithelial Cells by a New Transcellular Route Induced by Targeting ICAM-1

Rasa Ghaffarian<sup>a</sup>, Tridib Bhowmick<sup>b</sup>, and Silvia Muro<sup>a,b,\*</sup>

<sup>a</sup>Fischell Department of Bioengineering, 2330 Jeong H. Kim Engineering Building, University of Maryland, College Park, MD 20742, USA.

<sup>b</sup>Institute for Bioscience and Biotechnology Research, 5115 Plant Sciences Building, University of Maryland, College Park, MD 20742, USA.

### Abstract

Bioavailability of oral drugs, particularly large hydrophilic agents, is often limited by poor adhesion and transport across gastrointestinal (GI) epithelial cells. Drug delivery systems, such as sub-micrometer polymer carriers (nanocarriers, NCs) coupled to affinity moieties that target GI surface markers involved in transport, may improve this aspect. To explore this strategy, we coated 100-nm polymer particles with an antibody to ICAM-1 (a protein expressed on the GI epithelium and other tissues) and evaluated targeting, uptake, and transport in human GI epithelial cells. Fluorescence and electron microscopy, and radioisotope tracing revealed that anti-ICAM NCs specifically bound to cells in culture, were internalized via CAM-mediated endocytosis, trafficked by transcytosis across cell monolayers without disrupting the permeability barrier or cell viability, and enabled transepithelial transport of a model therapeutic enzyme ( $\alpha$ -galactosidase, deficient in lysosomal Fabry disease). These results indicate that ICAM-1 targeting may provide delivery of therapeutics, such as enzymes, to and across the GI epithelium.

### Keywords

ICAM-1; polymer nanocarriers; gastrointestinal epithelium; transcellular transport; enzyme delivery

### INTRODUCTION

Oral administration of therapeutics favors reduced cost, patient compliance, and flexible dosing [1]. However, implementation of this strategy poses challenges regarding drug bioavailability. This involves not only gastrointestinal (GI) degradation, which can be surmounted by encapsulation into protective materials, but also adhesion to the mucosa and transport across the GI tract [1].

Coupling of drugs to sub-micrometer carriers (nanocarriers, NCs) can help overcome these obstacles. NCs can be formulated with a variety of chemistries and structures: linear or

© 2012 Elsevier B.V. All rights reserved.

\*Correspondence should be addressed to: Silvia Muro, Institute for Bioscience and Biotechnology Research, 5115 Plant Sciences Building, University of Maryland, College Park, MD 20742-4450, Tel. 1+301-405-4777, Fax. 1+301-314-9075, muro@umd.edu.

**Publisher's Disclaimer:** This is a PDF file of an unedited manuscript that has been accepted for publication. As a service to our customers we are providing this early version of the manuscript. The manuscript will undergo copyediting, typesetting, and review of the resulting proof before it is published in its final citable form. Please note that during the production process errors may be discovered which could affect the content, and all legal disclaimers that apply to the journal pertain.

branched polymers, dendrimers, particles, micelles, liposomes, etc [2]. They can enhance drug solubility, protect against premature inactivation, optimize pharmacokinetics, and control release and metabolism [2]. Coupling of imaging agents to NCs further offers a means to visualize disease progression and therapeutic outcomes [3].

NCs also provide increased drug stability in the gut [4–7] and can be optimized for GI targeting and transport [4, 5, 8]. Targeting NCs to determinants expressed on the GI epithelium enhances bioadhesion, as shown for lectin-coated NCs or those that target cobalamin receptors on enterocytes [4, 8, 9]. Binding of NCs to specific cell-surface markers can induce transport into and/or across cells. Intracellular delivery of NCs is often mediated by targeting endocytic receptors, commonly associated with clathrin-coated pits or caveoli [10]. While endocytosis may direct NCs and their cargoes to intracellular compartments, it can also result in trafficking across the cell body with release at the basolateral side, a phenomenon known as transcellular transport or transcytosis [11]. Alternatively, drug carriers may elicit paracellular transport between the junctions that interlock adjacent cells, which also enhances access to the circulation [12–14].

A potential target of drug NCs in the intestinal mucosa is intercellular adhesion molecule-1 (ICAM-1), a transmembrane protein that serves as an anchor for leukocytes during inflammation [15, 16]. ICAM-1 is expressed predominantly on endothelial cells but also on most tissues, and is over-expressed in many pathological conditions [15, 16]. This enables drug targeting throughout the body, most favorably at disease sites, as shown for NCs administered systemically [17–19].

ICAM-1-specific affinity molecules, including antibodies (anti-ICAM) or affinity peptides, are being explored as therapeutics and targeting moieties in cell cultures, animal models, and clinical trials [17, 18, 20–22]. Binding of anti-ICAM-coated polymer NCs (anti-ICAM NCs) to ICAM-1 triggers cell adhesion molecule (CAM)-mediated endocytosis, a pathway distinct from classical clathrin and caveolar endocytosis, phagocytosis, and macropinocytosis [23]. Numerous studies have demonstrated delivery of therapeutic and imaging agents via this pathway [17, 18, 24–29]. Targeting and intracellular transport of anti-ICAM NCs can be modulated by parameters such as carrier size, shape, targeting valency, and bulk concentration [18, 30]. Particularly attractive, anti-ICAM NCs have shown promising intracellular delivery of large hydrophilic therapeutics, such as the enzymes used for replacement therapy of genetic lysosomal storage disorders (LSDs) [17, 18, 26, 31].

Since ICAM-1 is expressed on GI epithelial cells [15], it is also a viable target for drug delivery to, into, and/or across this tissue. Yet, the potential of this strategy for GI drug delivery has not been explored. In this work we describe efficient binding, internalization, and traffic of ICAM-1-targeted polymer NCs across GI epithelial cells, leading to significant transepithelial transport of a model enzyme,  $\alpha$ -galactosidase ( $\alpha$ -Gal), which is used for treatment of Fabry disease.

## METHODS

### Reagents

Mouse monoclonal antibody to human ICAM-1 (anti-ICAM) was R6.5 [16]. Goat polyclonal anti human occludin was from Santa Cruz Biotechnology (Santa Cruz, CA). Mouse immunoglobulin G (IgG) was from Calbiochem (San Diego, CA). Fluorescently-labeled secondary antibodies were from Jackson ImmunoResearch (West Grove, PA). FITC-labeled polystyrene beads were from Polysciences (Warrington, PA).  $\text{Na}^{125}\text{I}$  and Pierce Iodogen were from Perkin Elmer-Analytical Sciences (Wellesley, MA) and Thermo Scientific (Rockford, IL). All other reagents were from Sigma (St Louis, MO).

## Cell culture

Human epithelial colorectal adenocarcinoma Caco-2 cells (American Type Culture Collection, Manassas, VA) and T84 cells were cultured at 37° C, 5% CO<sub>2</sub>, and 95% humidity in DMEM medium (GibcoBRL, Grand Island, NY) supplemented with 4.50-g/L glucose, 15% fetal bovine serum (FBS) and antibiotics. For binding and uptake experiments, cells were seeded on 12-mm<sup>2</sup> gelatin-coated coverslips in 24-well plates. For transepithelial transport experiments, cells were grown on transwell filter inserts (polyethylene terephthalate, 0.4- $\mu$ m-pore size; BD Falcon, Franklin Lakes, NJ). When indicated, cells were incubated overnight with 10-ng/ml tumor necrosis factor- $\alpha$  (TNF- $\alpha$ ; BD Biosciences, Franklin Lakes, NJ) to mimic a pathological status.

## Preparation and characterization of nanocarriers

Fluorescent polystyrene beads (100-nm diameter) were coated by surface adsorption either with IgG or anti-ICAM, or a combination of anti-ICAM and  $\alpha$ -Gal (80:20 antibody-to-enzyme mass ratio), as described [26]. We used these particles as a model since our goal is to study their transport by Caco-2 cells and they have been previously shown to exert a performance similar to that of more clinically suitable ICAM-1-targeted poly(lactic-co-glycolic acid) (PLGA) nanoparticles in terms of targeting, endocytosis, intracellular trafficking, and enzyme delivery in cell culture models, as well as circulation, organ targeting, and enzyme delivery in mice [17, 19].

For radioisotope tracing, the antibody or enzyme (as indicated) were labeled with <sup>125</sup>Iodine [26]. Non-coated counterparts were separated by centrifugation, and coated NCs were resuspended using 1% bovine serum albumin (BSA) in phosphate buffer saline (PBS) and sonicated. As shown in Table 1, size, polydispersity, and  $\zeta$ -potential of coated and uncoated particles were measured by dynamic light scattering (Malvern, Worcestershire, UK), and the number of <sup>125</sup>I-antibody or <sup>125</sup>I-enzyme molecules on the particle surface was quantified using a gamma counter. In addition, release of <sup>125</sup>I- $\alpha$ -Gal from anti-ICAM NCs was assessed by separating the released enzyme fraction from the NC-bound fraction by centrifugation (13.8 g, 3-min), after incubation at 37° C from 15-min to 24-h in simulated gastric fluid (pH 1.2) or serum-supplemented cell media (pH 7.4).

## ICAM-1 expression and anti-ICAM nanocarrier binding to epithelial cells

ICAM-1 expression on quiescent versus TNF- $\alpha$  activated Caco-2 or quiescent T84 cells was verified after cell fixation with 2% paraformaldehyde, by immunostaining using anti-ICAM and a FITC-labeled secondary antibody. For binding studies, fixed cells (to avoid NC internalization) were incubated at room temperature with FITC-labeled anti-ICAM NCs or IgG NCs ( $2 \times 10^{10}$  particles/ml) for the indicated time, in the presence or absence of free anti-ICAM or control IgG. Non-bound particles were washed and cell nuclei were stained with 4',6-diamidino-2-phenylindole (DAPI). Samples were analyzed by fluorescence microscopy (settings described below), to quantify relative ICAM-1 expression over background fluorescence, or the number of NCs bound per cell, respectively.

## Internalization of anti-ICAM nanocarriers by epithelial cells

Quiescent versus TNF- $\alpha$ -activated Caco-2 or quiescent T84 cells were incubated with anti-ICAM NCs ( $2 \times 10^{10}$  particles/ml) at 37° C for 30-min to allow binding to the cell surface, followed by washing non-bound particles and incubation at 37° C for the indicated time to allow internalization. Experiments were conducted using control cell medium or medium containing 3-mM amiloride, 50- $\mu$ M monodansylcadaverine (MDC), or 1- $\mu$ g/ml filipin, to inhibit CAM-, clathrin-, or caveolin-mediated endocytosis [23]. Cells were fixed, incubated with Texas Red (TxR) goat anti-mouse IgG, and stained with DAPI to label nuclei. This

protocol renders NCs located on the cell surface double-labeled with TxR and FITC (red +green=yellow), while internalized NCs appear single-labeled in green FITC [23].

Samples were analyzed using Olympus IX81 fluorescence microscope (Olympus, Center Valley, PA) and a 40X PlanApo objective. Images were acquired using Orca-ER camera (Hamamatsu, Bridgewater, NJ) and analyzed with ImagePro 6.3 (Media Cybernetics, Silver Spring, MD). Internalization was calculated as the percentage of internalized NCs relative to the total amount of cell-associated particles [23].

### Effect of anti-ICAM nanocarriers on epithelial cell viability

Quiescent Caco-2 cells were incubated for 3-h at 37 °C in phenol-red-free cell media, either in the absence (control) or presence of anti-ICAM NCs. Then, non-bound particles were washed and the cell viability was assessed by staining cells with 1 μM calcein and 2 μM ethidium bromide (Live/Dead kit; Molecular Probes, Grand Island, NY). The samples were analyzed by fluorescence microscopy to quantify the percent of viable (calcein positive/ethidium negative) cells with respect to the total number of cells.

### Transepithelial transport of anti-ICAM nanocarriers and α-Gal cargo

Control or TNF-α-activated Caco-2 cells were grown to confluence onto 0.4-μm pore transwell filters. The status of the cell monolayer was assessed by measuring the transepithelial electrical resistance (TEER) using an EVOM™ volt-ohm meter and STX100 electrodes (World Precision Instruments, Sarasota, FL). Cells were fixed and tight junctions were immunostained with anti-occludin and a TxR-labeled secondary antibody. Confluent monolayers with TEER > 250Ω×cm<sup>2</sup> over background (16–21 days post-seeding), verified by the presence of tight junctions, were selected for experiments.

Control <sup>125</sup>I-IgG NCs, <sup>125</sup>I-anti-ICAM NCs, or anti-ICAM/<sup>125</sup>I-α-Gal NCs (56 nCi/ml) were added to the chamber above Caco-2 cells and incubated at 37° C for the indicated time intervals, either in the absence or presence of competing free IgG or anti-ICAM. The radioisotope content in the chamber above the cells (non-bound NCs), the chamber below the cells (transported NCs), and the cell fraction (bound and internalized NCs) was measured using a gamma counter. Free <sup>125</sup>Iodine released from NCs was determined by trichloroacetic acid (TCA) precipitation of each fraction, and this value was subtracted from calculations of the amount of NCs present in the samples. After subtraction, the number of NCs transported across the epithelial monolayer, the percentage of NCs transported with respect to the total number of NCs associated to the cells, and the apparent permeability coefficient (P<sub>app</sub>) were determined using the following equations,

$$\text{NCs transported} = \text{CPM}_{\text{basolateral}} \times (\text{NC}_{\text{added}} / \text{CPM}_{\text{added}})$$

$$\% \text{ NCs transported} = 100 \times [\text{CPM}_{\text{basolateral}} / (\text{CPM}_{\text{basolateral}} + \text{CPM}_{\text{cell fraction}})]$$

$$P_{\text{app}} \text{ (cm/s)} = (\text{CPM}_{\text{basolateral}} \times \text{Vol.}) / (A \times t \times \text{CPM}_{\text{added}})$$

where CPM are the <sup>125</sup>Iodine counts-per-minute added to the upper chamber (CPM<sub>added</sub>), the cell fraction (CPM<sub>cell fraction</sub>), or the lower chamber (CPM<sub>basolateral</sub>), and NC<sub>added</sub> are the number of NCs initially added to the upper chamber, A is the surface area of the filter membrane (cm<sup>2</sup>), Vol. is volume of medium in the upper chamber (ml), and t is time of incubation (s).

### Mechanism of transepithelial transport of anti-ICAM nanocarriers

Paracellular transport was assessed by evaluating leakage to the bottom chamber of <sup>125</sup>I-BSA (<sup>125</sup>I-Albumin) added above Caco-2 cells, in the presence of anti-ICAM NCs. This was compared to <sup>125</sup>I-Albumin transport in the absence of NCs, presence of IgG NCs, or in 5-

mM H<sub>2</sub>O<sub>2</sub> known to disrupt cell junctions. Transcellular transport of <sup>125</sup>I-anti-ICAM NCs, <sup>125</sup>I-IgG NCs, or <sup>125</sup>I-Albumin by a vesicular mechanism was assessed either in 50- $\mu$ M monodansylcadaverine (MDC; inhibitor of clathrin endocytosis), 1- $\mu$ g/ml filipin (inhibitor of caveolar endocytosis), 0.5- $\mu$ M wortmannin (inhibitor of phosphatidylinositol 3 kinase (PI3K), involved in macropinocytosis), or 20- $\mu$ M [5-(N-ethyl-N-isopropyl) amiloride] (EIPA, inhibitor of macropinocytosis and CAM-mediated endocytosis [23]). EIPA was used instead of amiloride since it more specifically inhibits the exchanger protein, NHE-1, involved in CAM-mediated transport. In all experiments, TEER was monitored before and after all incubations to assess the status of the permeability barrier.

Alternatively, for visualization purposes, samples were fixed with 2.5% glutaraldehyde in 0.1 M sodium cacodylate buffer and processed for transmission electron microscopy (TEM) from 80–90 nm thin resin-embedded sections as described [26].

### Statistical analysis

Data were calculated as mean $\pm$ standard error of the mean (S.E.M). Statistical significance was determined by Student's unpaired *t*-tests.

## RESULTS

### Targeting of anti-ICAM nanocarriers to gastrointestinal epithelial cells

We first verified ICAM-1 expression on T84 and Caco-2 cells grown on coverslips (Supplementary Figure 1). As described [32, 33], fluorescence microscopy revealed relative low and high ICAM-1 expression, respectively, on these cells: 62.8 $\pm$ 6.3-fold and 286.4 $\pm$ 9.5-fold over background. In Caco-2 cells expressing high levels of ICAM-1, TNF- $\alpha$  (mimicking cytokines typically present during GI pathological states) did not diminish ICAM-1 expression (109.4 $\pm$ 2.7% of quiescent cells; not shown). This cell type can therefore be used to study ICAM-1-mediated transport in quiescent versus disease-activated cells, without effecting ICAM-1 expression.

We then evaluated binding of FITC-labeled anti-ICAM NCs to activated Caco-2 cells (Figure 1), to compare to historical data on activated endothelial cells [19, 23, 26, 34]. Fluorescence microscopy revealed that binding of anti-ICAM NCs to fixed cells (to avoid internalization) was significant, e.g., 78.0 $\pm$ 4.1 NCs/cell at 30-min, which exceeded IgG NCs by 62.4 $\pm$ 6.2-fold. Binding was abolished by free anti-ICAM (97.6 $\pm$ 0.3% reduction) but not IgG (102.1 $\pm$ 2.6% of control) (Supplementary Figure 2). Anti-ICAM NCs bound to these cells at a similarly significant extent and rate relative to endothelial cells [19, 23, 26, 34], e.g., with 40.5 $\pm$ 2.7 NCs bound per cell as early as 5-min, a *t*<sub>1/2</sub> of 29-min, and binding saturation (*B*<sub>max</sub>) at 157 NCs/cell (Figure 1C). Binding was diminished (by 2.4 $\pm$ 0.3-fold), yet still significant in quiescent Caco-2 cells (32.1 $\pm$ 3.7 NCs/cell at 30-min; Supplementary Figure 3) and it was also detectable in quiescent T84 cells (14.0 $\pm$ 1.0 NCs/cell).

### Internalization of anti-ICAM nanocarriers by gastrointestinal epithelial cells

We then tested uptake of FITC-labeled anti-ICAM NCs by activated Caco-2 cells using an established technique that allows differential labeling of particles bound to the plasmalemma from those endocytosed [23] (Supplementary Figure 4A). Fluorescence microscopy indicated relatively rapid and efficient uptake of anti-ICAM NCs (Figure 2A): 50% after 22-min, ~80% after 1-h, and 98% at saturation, comparable to activated endothelial cells [19, 23, 26, 34]. A similar result was observed for quiescent Caco-2 cells (e.g., 95.2 $\pm$ 4.9% of activated cells at 1-h), and T84 cells (99.6 $\pm$ 2.7% of resting Caco-2 cells), despite their low level of NC binding (Supplementary Figure 4). This suggests that once an anti-ICAM NC



binds to ICAM-1, its endocytic rate is independent of the cell status and total number of NC bound, as in endothelial cells [19, 23, 26, 34].

To investigate the mechanism of uptake, internalization of anti-ICAM NCs was assessed using activated Caco-2 cells in the presence of MDC, filipin, or amiloride, which inhibit clathrin-, caveolar-, and CAM-mediated endocytosis [23]. As shown in Figure 2B and Supplementary Figure 5, amiloride reduced NC uptake by  $62.1 \pm 2.6\%$ , similar to endothelial cells [23] independently of binding (the total amount of cell-associated NCs in amiloride-treated cells was  $106.1 \pm 5.7\%$  of control; not shown). In contrast, filipin and MDC did not alter internalization of anti-ICAM NCs ( $97.1 \pm 2.2\%$  and  $95.9 \pm 2.1\%$  of control). Hence, endocytosis of anti-ICAM NCs by GI epithelial cells seemed to rely on the CAM-mediated pathway.

In addition, binding and uptake of anti-ICAM NCs for 3-h in Caco-2 cells did not cause any apparent cytotoxicity with respect to cells incubated in the absence of particles ( $98.8 \pm 0.1\%$  and  $99.1 \pm 0.2\%$  cell viability, respectively; data not shown).

### Validation of a cell model to study transepithelial transport

Caco-2 cells grown on porous transwell inserts exhibit the phenotype of mature enterocytes, including the presence of microvilli and tight junctions, dome formation, and production of brush border enzymes [33]. This system represents a well-established model of the human intestine to study transepithelial drug transport [35].

Caco-2 cells seeded on porous inserts formed a permeability barrier, assessed by measuring the transepithelial electrical resistance (TEER), whereby increased resistance to an electrical current indicates formation of epithelial junctions (Figure 3A). Cells plated at a density of  $1.5 \times 10^5$  cells/cm<sup>2</sup> reached confluence ~Day 12 and maintained monolayer integrity up to Day 18, indicated by TEER. This was validated by the presence of occludin-positive tight junctions (Figure 3B) in monolayers with high TEER ( $390\text{-}\Omega \times \text{cm}^2$ , Day 14), compared to poor tight junction labeling at low TEER ( $17\text{-}\Omega \times \text{cm}^2$ , Day 5). Neither TEER values nor occludin staining were affected by the addition of TNF- $\alpha$  to confluent cell monolayers at Day 14 (Figure 3C), to mimic disease-activation of the GI epithelium.

Finally, immunofluorescence confirmed ICAM-1 expression on Caco-2 cells following formation of a permeability barrier. Unlike cells cultured on coverslips, ICAM-1 distributed on microvilli inherent to polarized epithelial cells (Figure 3D), which remained unaffected by TNF- $\alpha$  activation (Supplementary Figure 6). This validated that Caco-2 cells display phenotypic features of mature enterocytes.

### Transport of anti-ICAM nanocarriers across gastrointestinal epithelial cells

Targeting and endocytosis of anti-ICAM NCs in GI epithelial cells are promising parameters to enhance drug delivery in pathological conditions affecting this tissue. If transport of anti-ICAM NCs occurred across this cellular barrier (an aspect never explored), this would also provide key preliminary information about potential future design of drug delivery carriers exploiting this path.

Using the quiescent Caco-2 cell monolayers described above, transport of <sup>125</sup>I-anti-ICAM NCs from the apical to the basolateral side of Caco-2 cells was surprisingly relevant: e.g., from  $85.0 \pm 11.3$  <sup>125</sup>I-anti-ICAM NCs transported/cell at 30-min to  $715.3 \pm 34.7$  NCs transported/cell at 24-h, equivalent to  $\sim 10^7$  NCs/cm<sup>2</sup> and  $\sim 10^8$  NCs/cm<sup>2</sup> of epithelial tissue (Figure 4A). This represented from  $28.0 \pm 3.7\%$  to  $41.2 \pm 1.9\%$  of all <sup>125</sup>I-anti-ICAM NCs associated to cells (Figure 4B). Transport of <sup>125</sup>I-anti-ICAM NCs was specific compared to control <sup>125</sup>I-IgG NCs ( $18.1 \pm 2.4$ -fold lower (Figure 4C) even at 24h, and significantly

inhibited in the presence of free anti-ICAM ( $16.7 \pm 3.2\%$  of control; Supplementary Figure 7) but not IgG ( $97.4 \pm 1.6\%$  of control). Transepithelial transport of  $^{125}\text{I}$ -anti-ICAM NCs was also found for TNF- $\alpha$ -activated Caco-2 cells (Table 2), demonstrating that this also occurs in GI epithelial cell models mimicking quiescent and pathological status.

The apparent permeability coefficient ( $P_{\text{app}}$ ), which represents the rate of transport and allows for comparison of permeability between different solutes (Methods), was  $2.1 \pm 0.2 \times 10^{-8}$  cm/s versus  $1.8 \pm 0.2 \times 10^{-9}$  cm/s for IgG NCs at 24-h (Figure 4D). Thus, in addition to intracellular transport (lysosomal trafficking) previously shown for anti-ICAM NCs, these NCs can also be transported across cells.

### Mechanism of transepithelial transport of anti-ICAM nanocarriers

Taking into account the reduced transepithelial flux of IgG NCs and inhibition of anti-ICAM NC traffic by free anti-ICAM, these results suggest that anti-ICAM NCs induce transport across GI epithelial cells, e.g., by a vesicular mechanism and/or opening of the cell junctions (transcellular versus paracellular transport).

We first tested the vesicular route. To minimize potential side effects that may affect the permeability barrier, we used EIPA. In contrast to amiloride, EIPA is more specific for  $\text{Na}^+/\text{H}^+$  exchanger NHE1 involved in CAM-mediated endocytosis [36]. As shown in Figure 5A, EIPA reduced transport of  $^{125}\text{I}$ -anti-ICAM NCs across cell monolayers by  $67.6 \pm 3.4\%$ , without affecting  $^{125}\text{I}$ -IgG NC transport or that of a control protein,  $^{125}\text{I}$ -Albumin ( $99.8 \pm 5.9\%$  and  $88.5 \pm 7.2\%$  of control; Supplementary Figure 8). Also, EIPA did not alter TEER values associated with the status of the cell junctions and the paracellular pathway (Supplementary Figure 9). In contrast, MDC and filipin did not inhibit transepithelial transport of  $^{125}\text{I}$ -anti-ICAM NCs, in accord with our internalization results. Since amiloride and EIPA inhibit both macropinocytosis and the CAM-mediated pathway, we evaluated wortmannin, an inhibitor of PI3K involved in macropinocytosis but not CAM-mediated endocytosis [23]. Wortmannin had no effect on  $^{125}\text{I}$ -anti-ICAM NC transport, confirming the nature of this pathway.

We then examined the paracellular route by evaluating potential changes in TEER during transport of anti-ICAM NCs across quiescent Caco-2 cells. As shown in Figure 5B, anti-ICAM NCs did not lower TEER over a period of 48-h (kept between  $88.8 \pm 2.0\%$  and  $101.0 \pm 5.8\%$  of control). This is in contrast to incubation with  $\text{H}_2\text{O}_2$ , which disrupts the permeability barrier [37] and caused a  $64.7 \pm 2.7\%$  decrease in TEER by 3-h and a reduction to background levels by 48-h.  $\text{H}_2\text{O}_2$  caused leakage of  $^{125}\text{I}$ -Albumin from the apical to the basolateral chamber ( $5.5 \pm 0.1$ -fold over control levels), whereas co-incubation with anti-ICAM NCs or IgG NCs did not increase  $^{125}\text{I}$ -Albumin transport (Figure 5C), in agreement with transcytosis of anti-ICAM NCs.

Finally, TEM permitted us to visualize anti-ICAM NCs bound to the surface of quiescent Caco-2 cell monolayers, on and between microvilli (black arrows; Figure 6A), internalized in large vesicular compartments within the cell body (black arrowheads; Figure 6B), and transcytosed between typical basolateral Caco-2 interdigitations (white arrows; Figure 6C), without disruption of tight junctions (white arrowheads; all panels in Figure 6).

### Transepithelial transport of $\alpha$ -galactosidase by anti-ICAM nanocarriers

We finally explored the potential of anti-ICAM NCs to transport a therapeutic cargo across Caco-2 monolayers. In our previous work, we have reported that anti-ICAM NCs efficiently target and deliver alpha-galactosidase ( $\alpha$ -Gal), to vascular endothelial cells in cell cultures and mice when injected systemically [26]. This enzyme is used as a replacement therapy for Fabry disease, a lysosomal storage disorder (LSD) caused by a genetic deficiency of  $\alpha$ -Gal.

In terms of stability of anti-ICAM NCs carrying  $\alpha$ -Gal, our previous study showed minimal enzyme release under storage conditions (1% BSA in PBS, pH 7.4, 4 °C) over a 3-day period and physiological-like fluids (serum-containing cell medium, pH 7.4, 37 °C) [26]. In the present study (Supplementary Figure 10), we additionally found minimal  $\alpha$ -Gal release from anti-ICAM NCs when incubated up to 24-h at 37 °C in simulated gastric fluid (pH 1.2): 10.2±0.8% release at 1-h and 22.3±1.6% release at 24-h. This is only slightly enhanced as compared to the enzyme release observed at pH 7.4, more reflective of intestinal conditions: 6.7±3.7% release at 1-h and 6.9±7.8% release at 24-h [26].

To evaluate whether an enzymatic payload can be transported across the GI epithelial barrier, we coated  $^{125}\text{I}$ - $\alpha$ -Gal onto anti-ICAM NCs as in our previous work [26] (see Methods) and tested transport using quiescent Caco-2 cell monolayers. Anti-ICAM/ $^{125}\text{I}$ - $\alpha$ -Gal NCs were transported across cells to a similar degree as anti-ICAM NCs (Table 3): 246.6±15.4 and 806.9±164.1 NCs transported per cell at 3-h and 24-h ( $P_{\text{app}}$  of 8.1±1.1 and 1.9±0.37×10<sup>-8</sup> cm/s). This represents 86.3±5.5% and 112.7±22.9% of the transport obtained in the case of enzyme-free anti-ICAM NCs. As a result, the amount of enzyme delivered across the epithelial barrier was substantial, e.g., 1.8±0.2×10<sup>5</sup> molecules of  $\alpha$ -Gal transported per cell at 3-h, which corresponds to ~10<sup>11</sup> molecules (4.9-ng) of enzyme per cm<sup>2</sup> tissue. Hence, anti-ICAM NCs satisfy the requirement of delivering a therapeutic agent relatively efficiently across a GI epithelial monolayer.

## DISCUSSION

Development of drugs aimed to reach the intestinal mucosa, either as a target for therapeutic intervention or a gatekeeper for transport into the circulation, is often hindered by poor adhesion to, and transport into and/or across the GI epithelial layer [1]. Whereas this represents less of an obstacle for small lipophilic compounds, it remains a major concern for hydrophilic therapeutics 100–200 Da in size [38].

A number of strategies have been designed to overcome this obstacle, including the use of affinity moieties that improve mucosal attachment, molecules that enhance GI permeability, and coupling to carriers that improve transepithelial transport [1, 4–7, 9, 14]. Several carrier formulations have proven beneficial in this regard [1, 4–7, 9, 14]. However, the ability of these strategies to deliver large hydrophilic agents into and/or across the GI epithelium, coupled to formulations that can target diseased sites after transport into the circulation, is a relatively unexplored area. In this work, we describe a strategy that utilizes ICAM-1 (a molecule that provides efficient biodistribution from the circulation [17, 19]) as a target on GI epithelial cells. This provides internalization of prototype polymer NCs within these cells and transcellular transport mediated by CAM endocytosis, without apparent alteration of the permeability barrier or cell viability, leading to transepithelial delivery of a model enzyme,  $\alpha$ -Gal (deficient in Fabry disease).

The number of anti-ICAM NCs bound to activated epithelial cells at saturation was half than that of endothelial cells (160 versus 300 NCs/cell) [19, 23, 26]. However, since the surface area of endothelial cells is 4–5-fold that of Caco-2 cells, this represents a significant targeting potential for GI tissue. Such a binding level is efficient for endothelial targeting *in vivo* [17, 18, 25, 26, 30]. Hence, similar binding in Caco-2 cells holds promise for targeting GI epithelium *in vivo*, where NCs will have a longer residence-time compared to the endothelium exposed to blood flow. Presence of ICAM-1 on microvilli of Caco-2 cells may further support targeting due to accessibility of these structures from the GI lumen.

We also detected binding of anti-ICAM NCs in quiescent cells, including T84 cells that express low ICAM-1 levels. This is encouraging since effective targeting by anti-ICAM



NCs has been reported *in vivo* for quiescent endothelium [17, 19, 30]. Low levels of ICAM-1 displayed on quiescent epithelial cells may suffice for significant targeting. This is useful for drug delivery to the GI epithelium for prophylactic interventions, or across this barrier for delivery to other sites. ICAM-1 expression is high in colorectal carcinoma, inflammatory bowel disease, Crohn's disease, ulcerative colitis, bacterial infections, and other conditions [15, 39–41]. Hence, ICAM-1 targeting also holds promise for therapeutic applications for these maladies.

Binding of anti-ICAM NCs to ICAM-1 on endothelial cells triggers CAM-mediated endocytosis, distinct from clathrin- and caveolar-mediated uptake, macropinocytosis and phagocytosis [23, 36]. Lack of dependence on PI3K signaling is also different from uptake of IgG-opsonized particles via Fcγ receptors [42]. This route provides intracellular delivery of therapeutics and imaging agents into the endothelium [17, 18, 24, 26, 29, 31, 36]. The finding that both quiescent and activated GI epithelial cells also employ this pathway is novel and indicates the potential of this strategy in the realm of drug delivery into intestinal tissue.

Beyond intracellular transport, anti-ICAM NCs were transported across epithelial monolayers. This is the first observation of such a feature related to CAM-mediated transport, sensitive to EIPA and specific blockage of ICAM-1 [23, 36]. Whether ICAM-1-mediated transcellular transport is unique to GI epithelial cells, needs to be elucidated. Previous work on endothelial cells has shown intracellular transport to endosomes and lysosomes [18, 26, 36]. This could be manipulated to favor carrier retention in pre-endosomal vesicles, endosomal/pre-lysosomal compartments, or redirect NCs to recycling pathways [43]. Those experiments used cells cultured on coverslips, which may preclude transport across cells. It is also possible that anti-ICAM NCs are transported across cells upon saturation of the lysosomal route. Yet, the plasticity demonstrated in terms of the chemistry, geometry of carriers, and cargo molecules that can efficiently use the CAM pathway over more restrictive vesicular mechanisms (e.g., clathrin, caveolar) [18], make this strategy particularly attractive to explore GI delivery using a variety of carrier formulations. One such formulation may include PLGA NCs, which have previously shown ICAM-1 targeting, CAM-mediated endothelial uptake, and intracellular trafficking in cell culture and animal models, similar to that of the model NCs used in this work [17, 19].

Transport of anti-ICAM NCs, though considerable ( $10^8$  NCs/cm<sup>2</sup> of epithelial surface at 24-h), did not decrease TEER or cause leakage of proteins (albumin) through the cell monolayer, which was remarkable given the relatively large (~160–180 nm) size of NCs versus that of albumin or electron currents. This supports the transcellular nature of ICAM-1-mediated transport, a relevant finding since paracellular mechanisms associated with intercellular junctions opening may increase passage of undesired substances across the intestinal barrier.

Transport of α-Gal across Caco-2 monolayers by ICAM-1-targeted NCs exemplifies delivery of a (protein) cargo by this strategy. NC-assisted transport of therapeutics in the GI has been mostly explored for small and poorly soluble drugs [44] or small polypeptides such as insulin [45], while delivery of large hydrophilic proteins by targeted NCs is relatively unexplored. Also, α-Gal represents a desirable enzyme replacement for LSDs, specifically Fabry disease. The possibility of designing replacement therapies for diseases characterized by enzyme deficiencies, represents an attractive opportunity to translate current systemic administration of these therapeutics into oral regimens, to reduce costs while increasing patient compliance.

Particularly in Fabry disease, intestinal pathology has been described, including deposition of glycosphingolipids (substrates for  $\alpha$ -Gal) in the intestinal wall, causing achalasia, malabsorption, diverticulosis, etc. [46]. Also, this disease is characterized by vasculopathy involving endothelial cells [46]. Delivery of  $\alpha$ -Gal by ICAM-1-targeted carriers may improve both intra-GI therapy and trans-GI transport into the circulation, where anti-ICAM NCs have been shown to enhance vascular delivery of  $\alpha$ -Gal [26]. Since the absorptive surface of the small intestine is  $\sim 200\text{--}250\text{ m}^2$ , presence of  $\alpha$ -Gal in the Caco-2 cell fraction ( $7.9\text{ ng/cm}^2$  at 3-h) and transport across this cellular barrier ( $4.9\text{ ng/cm}^2$ ) translates into a significant delivery capacity: 18-mg and 11-mg of  $\alpha$ -Gal into and across the GI, respectively, on the range of clinical doses ( $\sim 14\text{-mg}$  for a 70-kg person) [46].

The significant capacity of ICAM-1-targeting for protein (and likely drug) transport across epithelial cells highlights the promise of this approach in the context of GI delivery of therapeutics. Translation of this approach into animal models will require strategies to protect targeted carriers and their cargoes from degradation while in transit through the GI (e.g., due to low pH in the stomach and/or the presence of proteases), by encapsulation into protective materials with controlled release properties in areas where GI absorption occurs [47–49]. The relative low level of release of  $\alpha$ -Gal from anti-ICAM NCs (despite this sub-optimal, model formulation) found in this study under conditions mimicking the physiological temperature and pH in the gastric and intestinal compartments, is encouraging in moving forward our experimental efforts. Implementation of anti-ICAM NCs *in vivo* may also require strategies for overcoming the mucus barrier overlying the GI epithelium, which limits bioavailability of drug carriers by 1) decreasing residence time via continuous shedding and 2) inhibiting binding to the epithelial cell layer [50]. Yet, it is noteworthy that antibodies (such as the IgG type used in our study) and coated NCs (including polystyrene and other polymers) can diffuse through mucus due to a high charge density combined to a net neutral charge on their surface [50]. The same surface feature has been observed in mucus-penetrating pathogens, whose size is also comparable to that of NCs [50]. This may explain our recent observation that anti-ICAM NCs administered by oral gavage are capable to bind to duodenal epithelial cells in mice [51]. Other strategies to improve mucus penetration include surface modification with chitosan [52], polyethylene glycol (PEG) [53], surfactants [54], or mucolytic agents [50], which have been shown to enhanced penetration of polystyrene and PLGA particles up to 500 nm in size [53].

## CONCLUSIONS

Targeting of model polymer NCs to ICAM-1 on GI epithelial cells provides enhanced binding, uptake into, and transport across these cells. Intraepithelial uptake of ICAM-targeted NCs is regulated by CAM-mediated endocytosis as in endothelial cells, and this pathway is also involved in subsequent transepithelial transport of anti-ICAM NCs via vesicular transcytosis, without apparently affecting the permeability barrier or cell viability. This mechanism furthermore allows transport of a therapeutic enzyme,  $\alpha$ -Gal, into and across GI epithelial monolayers. Hence, ICAM-1-targeted NCs seem to hold promise as a relatively safe and efficient mode of drug delivery into and across the GI epithelium, particularly for large protein cargoes and likely other drugs with low bioavailability.

## Supplementary Material

Refer to Web version on PubMed Central for supplementary material.

## Acknowledgments

This work was supported by a fellowship of the Howard Hughes Medical Institute and National Science Foundation to R.G. and funds awarded to S.M. by the National Institutes of Health (Grant R01-HL98416) and the American Heart Association (Grant 09BGIA2450014). The authors thank Dr. Wenxia Song (Department of Cell Biology and Molecular Genetics, University of Maryland, College Park, MD) for kindly providing T84 cells and advice on the culturing conditions of these cells.

## REFERENCES

- Gabor F, Fillafer C, Neusch L, Ratzinger G, Wirth M. Improving oral delivery. *Handb Exp Pharmacol.* 2010; (197):345–398. [PubMed: 20217536]
- Torchilin V. Multifunctional and stimuli-sensitive pharmaceutical nanocarriers. *Eur J Pharm Biopharm.* 2009; 71(3):431–444. [PubMed: 18977297]
- Pan D, Carauthers SD, Chen J, Winter PM, SenPan A, Schmieder AH, Wickline SA, Lanza GM. Nanomedicine strategies for molecular targets with MRI and optical imaging. *Future Med Chem.* 2010; 2(3):471–490. [PubMed: 20485473]
- des Rieux A, Fievez V, Garinot M, Schneider YJ, Preat V. Nanoparticles as potential oral delivery systems of proteins and vaccines: a mechanistic approach. *J Control Release.* 2006; 116(1):1–27. [PubMed: 17050027]
- Cai Z, Wang Y, Zhu LJ, Liu ZQ. Nanocarriers: a general strategy for enhancement of oral bioavailability of poorly absorbed or pre-systemically metabolized drugs. *Curr Drug Metab.* 2010; 11(2):197–207. [PubMed: 20384585]
- Lamprecht A, Yamamoto H, Takeuchi H, Kawashima Y. Nanoparticles enhance therapeutic efficiency by selectively increased local drug dose in experimental colitis in rats. *J Pharmacol Exp Ther.* 2005; 315(1):196–202. [PubMed: 15980057]
- Serra L, Domenech J, Peppas NA. Engineering design and molecular dynamics of mucoadhesive drug delivery systems as targeting agents. *Eur J Pharm Biopharm.* 2009; 71(3):519–528. [PubMed: 18976706]
- Hamman JH, Demana PH, Olivier EI. Targeting Receptors, Transporters and Site of Absorption to Improve Oral Drug Delivery. *Drug Target Insights 2007(DTI-2-Hamman-et-al).* 2007
- Mishra N, Tiwari S, Vaidya B, Agrawal GP, Vyas SP. Lectin anchored PLGA nanoparticles for oral mucosal immunization against hepatitis B. *J Drug Target.* 2010
- Bareford LM, Swaan PW. Endocytic mechanisms for targeted drug delivery. *Adv Drug Deliv Rev.* 2007; 59(8):748–758. [PubMed: 17659804]
- Tuma PL, Hubbard AL. Transcytosis: crossing cellular barriers. *Physiol Rev.* 2003; 83(3):871–932. [PubMed: 12843411]
- Deli MA. Potential use of tight junction modulators to reversibly open membranous barriers and improve drug delivery. *Biochim Biophys Acta.* 2009; 1788(4):892–910. [PubMed: 18983815]
- Salama NN, Fasano A, Thakar M, Eddington ND. The impact of DeltaG on the oral bioavailability of low bioavailable therapeutic agents. *J Pharmacol Exp Ther.* 2005; 312(1):199–205. [PubMed: 15448170]
- El-Sayed M, Ginski M, Rhodes C, Ghandehari H. Transepithelial transport of poly(amidoamine) dendrimers across Caco-2 cell monolayers. *J Control Release.* 2002; 81(3):355–365. [PubMed: 12044574]
- Muro, S. *Endothelial Biomedicine.* Aird, WC., editor. New York: Cambridge University Press; 2007. p. 1058-1070.
- Marlin SD, Springer TA. Purified intercellular adhesion molecule-1 (ICAM-1) is a ligand for lymphocyte function-associated antigen 1 (LFA-1). *Cell.* 1987; 51(5):813–819. [PubMed: 3315233]
- Garnacho C, Dhama R, Simone E, Dziubla T, Leferovich J, Schuchman EH, Muzykantov V, Muro S. Delivery of acid sphingomyelinase in normal and niemann-pick disease mice using intercellular adhesion molecule-1-targeted polymer nanocarriers. *J Pharmacol Exp Ther.* 2008; 325(2):400–408. [PubMed: 18287213]

18. Muro S, Garnacho C, Champion JA, Leferovich J, Gajewski C, Schuchman EH, Mitragotri S, Muzykantov VR. Control of endothelial targeting and intracellular delivery of therapeutic enzymes by modulating the size and shape of ICAM-1-targeted carriers. *Mol Ther*. 2008; 16(8):1450–1458. [PubMed: 18560419]
19. Muro S, Dziubla T, Qiu W, Leferovich J, Cui X, Berk E, Muzykantov VR. Endothelial targeting of high-affinity multivalent polymer nanocarriers directed to intercellular adhesion molecule 1. *J Pharmacol Exp Ther*. 2006; 317(3):1161–1169. [PubMed: 16505161]
20. Zimmerman T, Blanco FJ. Inhibitors targeting the LFA-1/ICAM-1 cell-adhesion interaction: design and mechanism of action. *Curr Pharm Des*. 2008; 14(22):2128–2139. [PubMed: 18781967]
21. Villanueva FS, Jankowski RJ, Klivanov S, Pina ML, Alber SM, Watkins SC, Brandenburger GH, Wagner WR. Microbubbles targeted to intercellular adhesion molecule-1 bind to activated coronary artery endothelial cells. *Circulation*. 1998; 98(1):1–5. [PubMed: 9665051]
22. Haug CE, Colvin RB, Delmonico FL, Auchincloss H Jr, Tolkoff-Rubin N, Preffer FI, Rothlein R, Norris S, Scharshmidt L, Cosimi AB. A phase I trial of immunosuppression with anti-ICAM-1 (CD54) mAb in renal allograft recipients. *Transplantation*. 1993; 55(4):766–772. discussion 772–763. [PubMed: 8097341]
23. Muro S, Wiewrodt R, Thomas A, Koniaris L, Albelda SM, Muzykantov VR, Koval M. A novel endocytic pathway induced by clustering endothelial ICAM-1 or PECAM-1. *J Cell Sci*. 2003; 116(Pt 8):1599–1609. [PubMed: 12640043]
24. Finikova OS, Lebedev AY, Aprelev A, Troxler T, Gao F, Garnacho C, Muro S, Hochstrasser RM, Vinogradov SA. Oxygen microscopy by two-photon-excited phosphorescence. *Chemphyschem*. 2008; 9(12):1673–1679. [PubMed: 18663708]
25. Murciano JC, Muro S, Koniaris L, Christofidou-Solomidou M, Harshaw DW, Albelda SM, Granger DN, Cines DB, Muzykantov VR. ICAM-directed vascular immunotargeting of antithrombotic agents to the endothelial luminal surface. *Blood*. 2003; 101(10):3977–3984. [PubMed: 12531816]
26. Hsu J, Serrano D, Bhowmick T, Kumar K, Shen Y, Kuo YC, Garnacho C, Muro S. Enhanced Endothelial Delivery and Biochemical Effects of alpha-Galactosidase by ICAM-1-Targeted Nanocarriers for Fabry Disease. *J Control Release*. 2011; 149(3):323–331. [PubMed: 21047542]
27. Chittasupho C, Xie SX, Baoum A, Yakovleva T, Siahaan TJ, Berkland CJ. ICAM-1 targeting of doxorubicin-loaded PLGA nanoparticles to lung epithelial cells. *Eur J Pharm Sci*. 2009; 37(2): 141–150. [PubMed: 19429421]
28. Weller GE, Villanueva FS, Klivanov AL, Wagner WR. Modulating targeted adhesion of an ultrasound contrast agent to dysfunctional endothelium. *Ann Biomed Eng*. 2002; 30(8):1012–1019. [PubMed: 12449762]
29. Rossin R, Muro S, Welch MJ, Muzykantov VR, Schuster DP. In vivo imaging of <sup>64</sup>Cu-labeled polymer nanoparticles targeted to the lung endothelium. *J Nucl Med*. 2008; 49(1):103–111. [PubMed: 18077519]
30. Calderon AJ, Bhowmick T, Leferovich J, Burman B, Pichette B, Muzykantov V, Eckmann DM, Muro S. Optimizing endothelial targeting by modulating the antibody density and particle concentration of anti-ICAM coated carriers. *J Control Release*. 2011; 150(1):37–44. [PubMed: 21047540]
31. Hsu J, Northrup L, Bhowmick T, Muro S. Enhanced delivery of alpha-glucosidase for Pompe disease by ICAM-1-targeted nanocarriers: comparative performance of a strategy for three distinct lysosomal storage disorders. *Nanomedicine*. 2011
32. Kaiserlian D, Rigal D, Abello J, Revillard JP. Expression, function and regulation of the intercellular adhesion molecule-1 (ICAM-1) on human intestinal epithelial cell lines. *Eur J Immunol*. 1991; 21(10):2415–2421. [PubMed: 1680698]
33. Hidalgo IJ, Raub TJ, Borchardt RT. Characterization of the human colon carcinoma cell line (Caco-2) as a model system for intestinal epithelial permeability. *Gastroenterology*. 1989; 96(3): 736–749. [PubMed: 2914637]
34. Muro S, Gajewski C, Koval M, Muzykantov VR. ICAM-1 recycling in endothelial cells: a novel pathway for sustained intracellular delivery and prolonged effects of drugs. *Blood*. 2005; 105(2): 650–658. [PubMed: 15367437]

35. Skolnik S, Lin X, Wang J, Chen XH, He T, Zhang B. Towards prediction of in vivo intestinal absorption using a 96-well Caco-2 assay. *J Pharm Sci.* 2010; 99(7):3246–3265. [PubMed: 20166204]
36. Muro S, Mateescu M, Gajewski C, Robinson M, Muzykantov VR, Koval M. Control of intracellular trafficking of ICAM-1-targeted nanocarriers by endothelial Na<sup>+</sup>/H<sup>+</sup> exchanger proteins. *Am J Physiol Lung Cell Mol Physiol.* 2006; 290(5):L809–L817. [PubMed: 16299052]
37. Ward PD, Tippin TK, Thakker DR. Enhancing paracellular permeability by modulating epithelial tight junctions. *Pharm Sci Technol Today.* 2000; 3(10):346–358. [PubMed: 11050459]
38. Camenisch G, Alsenz J, van de Waterbeemd H, Folkers G. Estimation of permeability by passive diffusion through Caco-2 cell monolayers using the drugs' lipophilicity and molecular weight. *Eur J Pharm Sci.* 1998; 6(4):317–324. [PubMed: 9795088]
39. Bowen-Yacyshyn MB, Bennett CF, Nation N, Rayner D, Yacyshyn BR. Amelioration of chronic and spontaneous intestinal inflammation with an antisense oligonucleotide (ISIS 9125) to intracellular adhesion molecule-1 in the HLA-B27/beta2 microglobulin transgenic rat model. *J Pharmacol Exp Ther.* 2002; 302(3):908–917. [PubMed: 12183646]
40. Hopkins AM, Baird AW, Nusrat A. ICAM-1: targeted docking for exogenous as well as endogenous ligands. *Adv Drug Deliv Rev.* 2004; 56(6):763–778. [PubMed: 15063588]
41. Vainer B. Intercellular adhesion molecule-1 (ICAM-1) in ulcerative colitis: presence, visualization, and significance. *APMIS.* 2010; 118(Suppl 129):1–43. [PubMed: 20041868]
42. Huang ZY, Barreda DR, Worth RG, Indik ZK, Kim MK, Chien P, Schreiber AD. Differential kinase requirements in human and mouse Fc-gamma receptor phagocytosis and endocytosis. *J Leukoc Biol.* 2006; 80(6):1553–1562. [PubMed: 16921024]
43. Muro, S.; Muzykantov, V. *Organelle-specific pharmaceutical nanotechnology.* Weissig, V.; D'Souza, GGM., editors. Hoboken, NJ: John Wiley & Sons; 2010. p. 449-474.
44. Fahr A, Liu X. Drug delivery strategies for poorly water-soluble drugs. *Expert Opin Drug Deliv.* 2007; 4(4):403–416. [PubMed: 17683253]
45. Dange C, Reis CP, Maincent P. Nanoparticle strategies for the oral delivery of insulin. *Expert Opin Drug Deliv.* 2008; 5(1):45–68. [PubMed: 18095928]
46. Desnick, RJ.; Ioannou, YA.; Eng, CM. *The Metabolic and Molecular Bases of Inherited Disease.* Scriver, C.; Beaudet, A.; Sly, W.; Valle, D.; Childs, B.; Kinzler, K.; Vogelstein, B., editors. McGraw-Hill; 2001.
47. Park K, Kwon IC, Park K. Oral protein delivery: Current status and future prospect. *React Funct Polym.* 2011; 71(3):280–287.
48. Kamei N, Morishita M, Chiba H, Kavimandan NJ, Peppas NA, Takayama K. Complexation hydrogels for intestinal delivery of interferon beta and calcitonin. *J Control Release.* 2009; 134(2): 98–102. [PubMed: 19095021]
49. Sharma M, Sharma V, Panda AK, Majumdar DK. Development of enteric submicron particle formulation of papain for oral delivery. *Int J Nanomedicine.* 2011; 6:2097–2111. [PubMed: 22114474]
50. Lai SK, Wang YY, Hanes J. Mucus-penetrating nanoparticles for drug and gene delivery to mucosal tissues. *Adv Drug Deliv Rev.* 2009; 61(2):158–171. [PubMed: 19133304]
51. Mane V, Muro S. Biodistribution and endocytosis of ICAM-1-targeting antibodies and nanocarriers in the gastrointestinal tract in mice. *Int J Nanomedicine.* (Revised manuscript under consideration).
52. Prego C, Torres D, Alonso MJ. The potential of chitosan for the oral administration of peptides. *Expert Opin Drug Deliv.* 2005; 2(5):843–854. [PubMed: 16296782]
53. Lai SK, O'Hanlon DE, Harrold S, Man ST, Wang YY, Cone R, Hanes J. Rapid transport of large polymeric nanoparticles in fresh undiluted human mucus. *Proc Natl Acad Sci U S A.* 2007; 104(5):1482–1487. [PubMed: 17244708]
54. Mura S, Hillaireau H, Nicolas J, Kerdine-Romer S, Le Droumaguet B, Delomenie C, Nicolas V, Pallardy M, Tsapis N, Fattal E. Biodegradable nanoparticles meet the bronchial airway barrier: how surface properties affect their interaction with mucus and epithelial cells. *Biomacromolecules.* 2011; 12(11):4136–4143. [PubMed: 21981120]



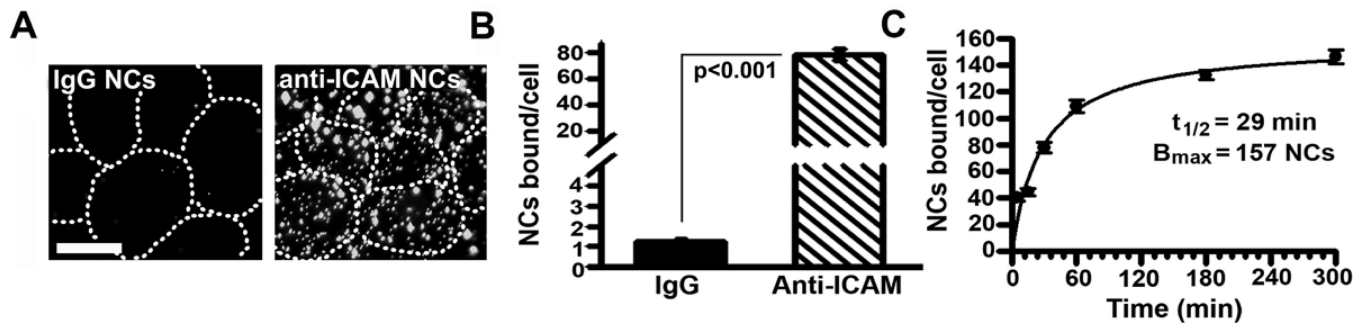


**Figure 1. Binding of anti-ICAM nanocarriers to Caco-2 cells**

(A) Fluorescence microscopy of fixed TNF- $\alpha$ -activated Caco-2 cells incubated with FITC-labeled anti-ICAM NCs or control IgG NCs (30-min, room temperature). Dashed lines mark the cell borders, observed by phase-contrast. Magnification bar=10- $\mu\text{m}$ . (B) Images were analyzed to quantify NCs bound per cell. (C) The binding kinetics of anti-ICAM NCs was determined at the indicated times and fit by non-linear regression ( $r^2=0.98$ ). Data are means  $\pm$ S.E.M. (n = 20 cells from 2 experiments).

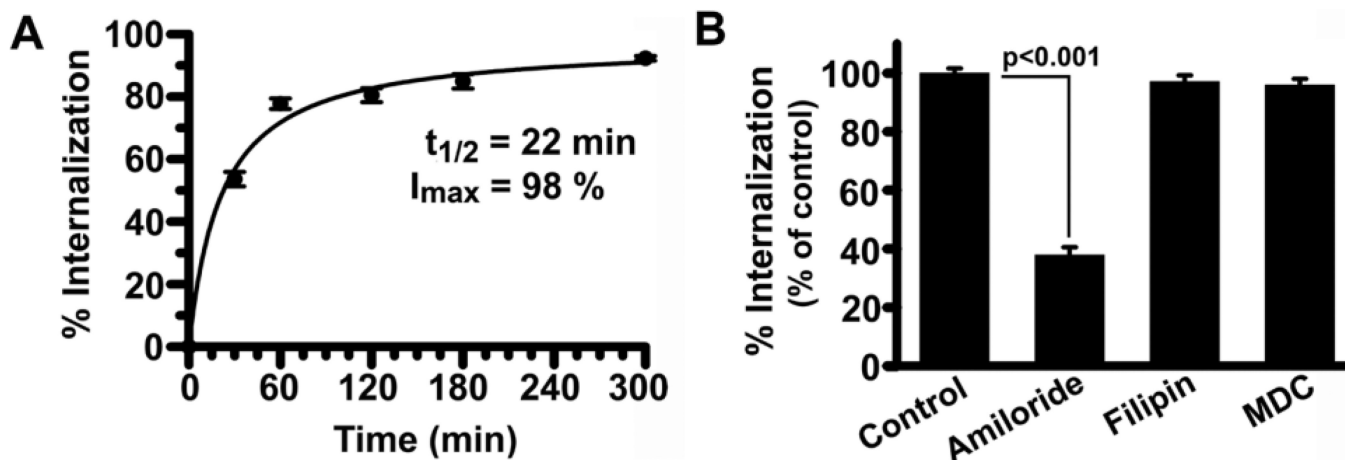


**Figure 2. CAM-mediated endocytosis of anti-ICAM nanocarriers by Caco-2 cells**  
 (A) TNF- $\alpha$ -activated cells were incubated with FITC-labeled anti-ICAM NCs for 30-min to allow binding, non-bound carriers were washed, and cells were incubated for varying times at 37°C to allow internalization. After cell fixation, surface-bound NCs were stained with a TxR-labeled secondary antibody. Fluorescence microscopy was used to analyze the fraction of single-labeled green (internalized) NCs to double-labeled green+red (yellow, surface-bound) NCs. The data were fit by non-linear regression ( $r^2=0.99$ ). (B) Internalization of anti-ICAM NCs (1 h) was assessed in the presence of 3-mM amiloride, 50- $\mu$ M MDC, or 1- $\mu$ g/ml filipin, and data was normalized to control. Data are means $\pm$ S.E.M. (n = 20 cells from 2 experiments).

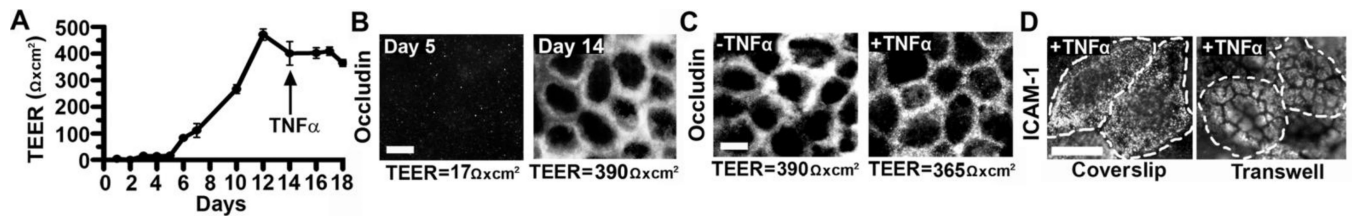


### Figure 3. Caco-2 monolayers as a model for transepithelial transport

Caco-2 cells were grown on permeable membrane inserts (0.4- $\mu\text{m}$  pore) at  $1.5 \times 10^5$  cells/ $\text{cm}^2$ . (A) Transepithelial electrical resistance (TEER) was measured to assess monolayer integrity. Cells were treated with TNF- $\alpha$  on Day 14. Data are means  $\pm$  S.E.M. (n=3). (B) Fluorescence microscopy of tight junctions immunolabeled with anti-occludin and TxR secondary antibody on Days 5 or 14 (low versus high TEER values, respectively). (C) Comparison of control versus TNF- $\alpha$ -activated cells stained for tight junctions as in (B). (D) Fluorescence microscopy comparing ICAM-1 immunostaining of TNF- $\alpha$ -activated, confluent Caco-2 cells either grown on coverslips or transwell inserts. The dashed lines mark the cell borders, observed by phase-contrast. Magnification bar=10  $\mu\text{m}$ .

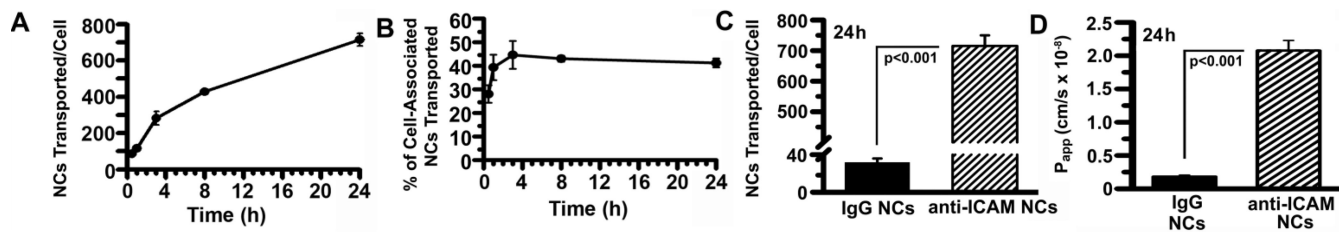


#### Figure 4. Transport of anti-ICAM nanocarriers across Caco-2 cell monolayers

Confluent non-activated Caco-2 monolayers grown on transwell inserts were incubated with  $^{125}\text{I}$ -anti-ICAM NCs or  $^{125}\text{I}$ -IgG NCs added to the apical chamber. (A–C)  $^{125}\text{I}$  content in the basolateral chamber was measured at the indicated time points, to calculate the amount of NCs transported per cell (see Methods). (B) Percent of transported NCs was calculated as the ratio of carriers found in the basolateral fraction to that in the combined basolateral and cell fractions. (D) Apparent permeability coefficients ( $P_{app}$ ) were calculated as described in Methods from the rates of transport of  $^{125}\text{I}$ -anti-ICAM NCs or  $^{125}\text{I}$ -IgG NCs. Data are shown as means  $\pm$  S.E.M. (n=4).

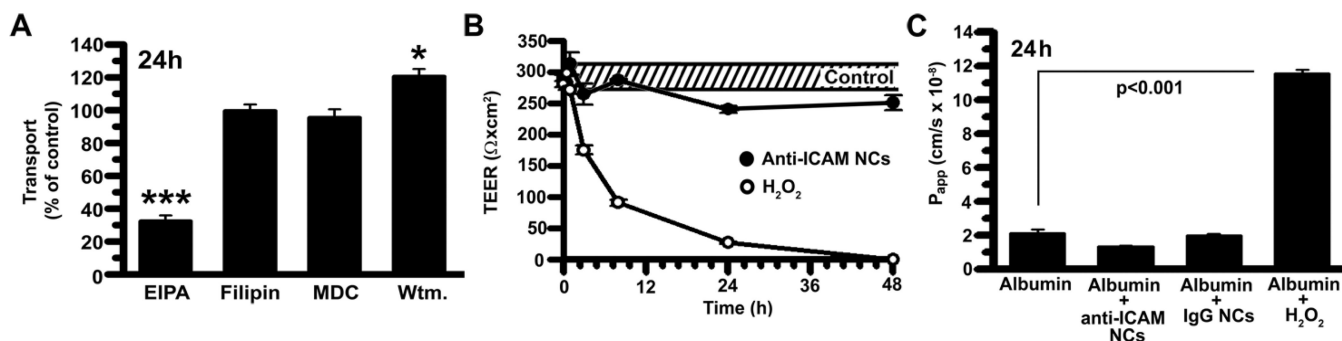


**Figure 5. Mechanism of transport of anti-ICAM nanocarriers across Caco-2 cells**

(A) Transcellular transport of <sup>125</sup>I-anti-ICAM NCs across confluent, non-activated Caco-2 cells was assessed at 24-h (described in Fig. 4) in the absence or presence of 20- $\mu$ M EIPA, 1- $\mu$ g/ml filipin, 50- $\mu$ M MDC, or 0.5- $\mu$ M wortmannin. (B) TEER was measured during transport of <sup>125</sup>I-anti-ICAM NCs across Caco-2 cells, to assess paracellular transport. TEER values in the absence of NCs are shown as controls (the dashed interval marks S.E.M of the mean value). Incubation with 5-mM H<sub>2</sub>O<sub>2</sub> is a positive control for opening of intercellular junctions. (C) Paracellular protein leakage, measured as the apparent permeability coefficient (P<sub>app</sub>) of <sup>125</sup>I-Albumin crossing the cell monolayer in the absence or presence of 5-mM H<sub>2</sub>O<sub>2</sub>, IgG NCs, or anti-ICAM NCs, was measured and calculated as in Fig. 4. Data are shown as means  $\pm$  S.E.M. (n = 4).



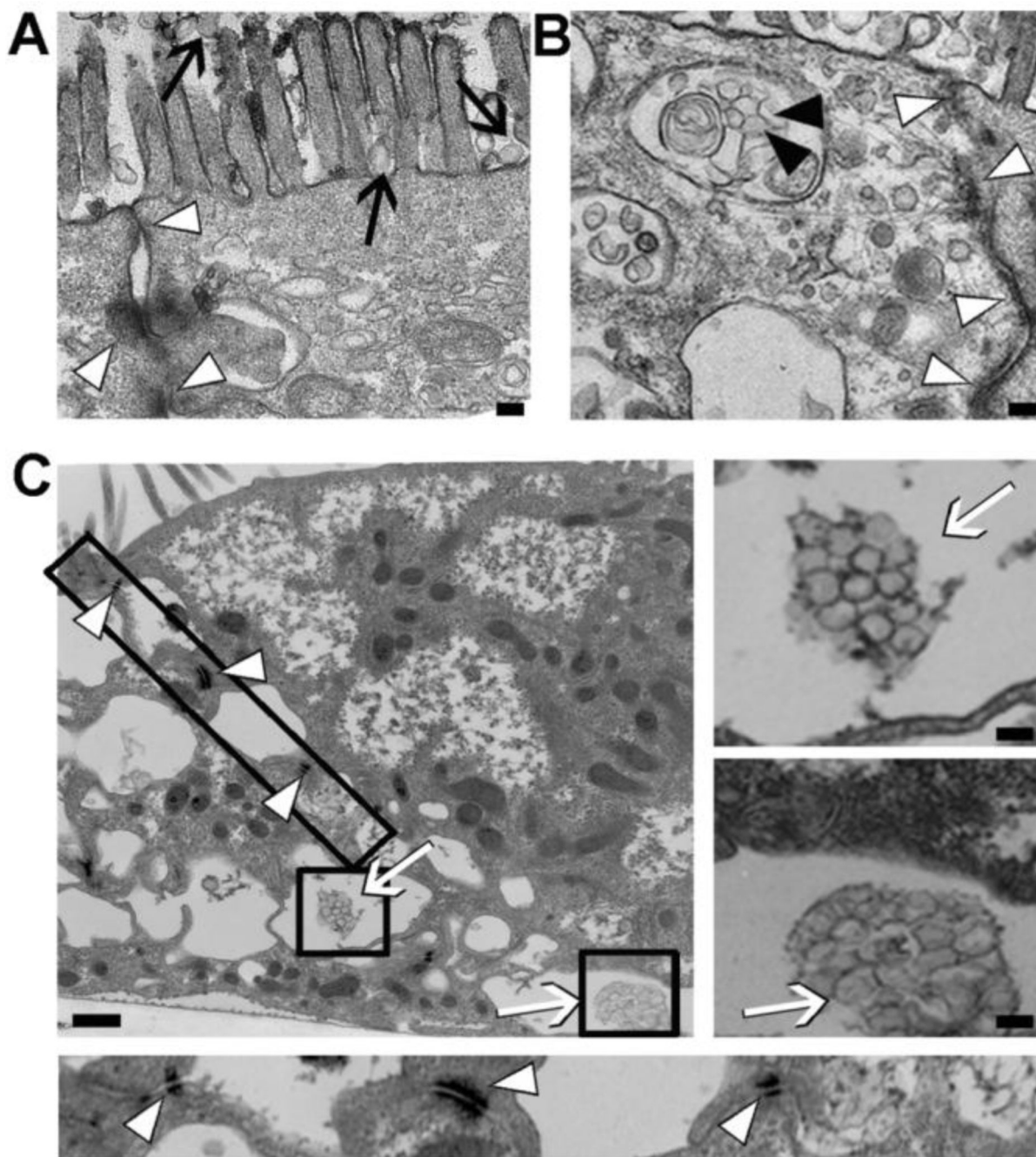


**Figure 6. Visualization of transport of anti-ICAM nanocarriers across Caco-2 cells**  
 Transmission electron micrographs of anti-ICAM NCs incubated for 3-h with non-activated Caco-2 cells. Images show anti-ICAM NCs (A) bound (black arrows), (B) internalized within vesicular compartments (black arrowheads), and (C) transcytosed to the basolateral space between cells (white arrows), with intact cell junctions (white arrowheads). The boxes represent areas further magnified in independent panels. Magnification bar=100-nm.

Table 1

Nanocarrier characterization.

	Size (nm)	Polydispersity	Z-potential (mV)	Antibody molecules/NC	Enzyme molecules/NC
Uncoated NCs	167.0 ± 1.2	0.114 ± 0.009	-13.7 ± 0.2	-	-
IgG NCs	279.7 ± 1.2	0.219 ± 0.014	-9.5 ± 0.4	149.7 ± 10.7	-
Anti-ICAM NCs	258.5 ± 11.3	0.220 ± 0.048	-12.9 ± 0.4	208.3 ± 42.7	-
Anti-ICAM/ $\alpha$ -Gal NCs	230.0 ± 1.1	0.186 ± 0.008	-12.9 ± 0.4	158.0 ± 1.1	195.4 ± 58.0

NCs = nanocarriers,  $\alpha$ -Gal =  $\alpha$ -galactosidase. Data are shown as means  $\pm$  S.E.M. (n = 3)

Table 2

Trans epithelial transport of anti-ICAM nanocarriers.

	Total NCs associated/cell	Intracellular NCs/cell	NCs transported /cell	% Transported	$P_{app}$ (cm/s $\times 10^{-8}$ )
<b>- TNF-<math>\alpha</math></b>					
<b>3h</b>	873.9 $\pm$ 138.4	546.2 $\pm$ 123.0	282.2 $\pm$ 37.5	44.6 $\pm$ 5.9	13.2 $\pm$ 0.3
<b>24 h</b>	2798.1 $\pm$ 172.7	1587.6 $\pm$ 218.4	715.3 $\pm$ 34.7	41.2 $\pm$ 1.9	2.1 $\pm$ 0.5
<b>+ TNF-<math>\alpha</math></b>					
<b>3h</b>	1331.2 $\pm$ 232.5	985.1 $\pm$ 198.1	346.1 $\pm$ 54.3	27.0 $\pm$ 3.4	7.2 $\pm$ 1.1
<b>24 h</b>	2768.1 $\pm$ 745.2	2244.6 $\pm$ 734.3	523.5 $\pm$ 20.0	30.2 $\pm$ 6.7	1.4 $\pm$ 0.1

NCs = nanocarriers; Total NCs associated/cell = NCs in the cell fraction/number of cell + NCs transported/number of cells; % Transported =  $100 \times (\text{NCs transported} / \text{Total NCs associated})$ ;  $P_{app}$  = apparent permeability coefficient (cm/s). See Methods for further description of these parameters. Data are shown as means  $\pm$  S.E.M. (n = 4 wells).

Table 3

Trans epithelial transport of  $\alpha$ -Gal by anti-ICAM NCs

	Total NCs associated/cell	Intracellular NCs/cell	Transported NCs/cell	% Transported	Transported $\alpha$ -Gal molecules/cell $\times 10^5$	pg transported/cell $\times 10^{-3}$	$P_{app}$ ( $\times 10^{-8}$ cm/s)
<b>3h</b>	663.4 $\pm$ 116.0	434.0 $\pm$ 76.8	243.6 $\pm$ 15.4	44.4 $\pm$ 6.7	1.8 $\pm$ 0.2	9.7 $\pm$ 1.2	8.1 $\pm$ 1.1
<b>24h</b>	2024.8 $\pm$ 409.3	1218.9 $\pm$ 255.6	806.9 $\pm$ 164.1	40.6 $\pm$ 2.0	3.9 $\pm$ 0.5	21.3 $\pm$ 2.5	1.9 $\pm$ 0.4

NCs = nanocarriers;  $\alpha$ -Gal =  $\alpha$ -galactosidase; Total NCs associated/cell = NCs in the cell fraction/number of cell + NCs transported/number of cell; % Transported =  $100 \times$  (NCs transported / Total NCs associated);  $P_{app}$  = apparent permeability coefficient (cm/s). See Methods for further description of these parameters. Data were obtained in quiescent Caco-2 cells, and represent means  $\pm$  S.E.M. (n = 8 wells).